Cellulose (2023) 30:6679–6694
https://doi.org/10.1007/s10570-023-05287-5

ORIGINAL RESEARCH

# Flame-retardant, antibacterial and hydrophobic multifunctional coatings on cotton fabrics via layer-by-layer self-assembly

**Xiaoyan Chen · Fang Ding · Shumin Zhang · Ying Liu · Xiuliang Hou · Xuehong Ren**

Received: 21 December 2022 / Accepted: 24 May 2023 / Published online: 30 May 2023


**Abstract** The development of multifunctional fabrics remains a necessity of high priority to meet the growing requirements in practical applications. However, developing flame retardant fabrics with antibacterial property and hydrophobicity still faces many challenges. In this study, novel multifunctional cotton fabrics with flame retardancy, antibacterial property, and hydrophobicity were successfully prepared by layer-by-layer (LBL) self-assembly. A novel flame retardant and antibacterial linear polymer P(AA-ADMH) containing a nitrogen flame-retardant and an antibacterial based on *N*-halamine was synthesized. To obtain versatile functionalities, P(AA-ADMH), phytic acid (PA), and γ-aminopropyl triethoxysilane (APS) were introduced to cotton fabrics by LBL self-assembly. The limiting oxygen index (LOI) of the modified cotton fabrics increased to 27.3%, and the peak of heat release rate (PHRR) decreased by 29.3%. Due to the presence of *N*-halamine structure, the modified cotton fabrics exhibited significant antibacterial efficacy within 30 min. In addition, the contact angle of the modified cotton fabrics was around 110° which could reduce the adhesion of bacteria on the modified fabrics. This study provides a novel method to potentially develop multifunctional cellulose textiles for the fields of fire safety and other protection.

**Keywords** Multifunctional cotton fabrics · Flame retardant · Antibacterial · Hydrophobic · Layer-by-layer

## Introduction

As an important bio-based textile, cotton fabric has been widely used for home decoration, packaging and clothing, due to their excellent properties of water absorptivity, flexibility, wearing comfort, breathability, and biodegradation (Li et al. 2020; Makhlouf et al. 2021; Nabipour et al. 2020; Zhang et al. 2022). However, cotton fabrics were highly flammable, increasing the risk of fire events in everyday life and causing hazards to both people's health and property safety (Wang et al. 2020, 2021a). To imparting flame retardancy to cotton fabrics, many technologies have been reported, such as impregnating, coating (Zhang et al.

**Supplementary Information** The online version contains supplementary material available at https://doi.org/10.1007/s10570-023-05287-5.

X. Chen · F. Ding · S. Zhang · Y. Liu · X. Hou (✉)
Key Laboratory of Eco-Textiles of Ministry of Education, College of Textile Science and Engineering, Jiangnan University, Wuxi 214122, Jiangsu, China
e-mail: houxl@jiangnan.edu.cn

X. Ren (✉)
Key Laboratory of Textile Fiber and Products, Ministry of Education, Hubei International Scientific and Technological Cooperation Base of Intelligent Textile Materials & Application, School of Textile Science and Engineering, Wuhan Textile University, Wuhan 430200, Hubei, China
e-mail: xuehongr@hotmail.com

2017), surface grafting treatment (Wang et al. 2018b; Zhang et al. 2018), sol–gel technique (Bentis et al. 2019), and layer-by-layer (LBL) self-assembly (Pan et al. 2018). Among them, due to flexibility within the kinds of components, the LBL self-assembly method has been widely applied with modified systems which containing various components. Li et al. (2019a, b) synthesized a novel compound contained silicon and nitrogen, and combined the compound with phytic acid (PA) to fabricate flame retardant and antibacterial cotton fabrics through LBL self-assembly method (Li et al. 2019b). In recent years, researchers have focused on designing and developing highly effective flame retardants without halogen for safety and environmental-friendly considerations. According to published literature, phosphorus-, silicon- or nitrogen- compound based flame retardants represent replacement to halogen-based flame retardants (Li et al. 2022). Wang et al. (2021b) manufactured flame retardant cotton fabrics with the synthetic EPSO-P containing phosphorus (P), nitrogen (N) and silicon (Si), and the LOI of treated fabrics reached to 31.4% (Wang et al. 2021b). Manfredia et al. (2018) synthesized eight linear polyamidoamines (PAAs), and proved the potential of PAAs as flame retardants for cotton textiles (Manfredi et al. 2018). Many PAAs are water-soluble and hold great promise for ecof-riendly flame-retardants (Arioli et al. 2020).

The breathability and polysaccharide structure of cellulose are a natural culture medium for bacterial proliferation, which limits the application of cotton fabrics in areas where safety requirements are high (Mu et al. 2018). For antibacterial modification, quaternary ammonium salts, guanidine, metal ions, *N*-halamine compounds, and nanoparticles have been widely used to prepare antibacterial compounds. *N*-halamine compounds are extensively been explored for such due to their advantages of antimicrobial efficacies in a short time, long-term stability, broad-spectrum activity, low toxicity and regeneration ability (Tian et al. 2021; Xu et al. 2021). Various *N*-halamine copolymers which are applied as antibacterial textile coatings have been reported (Zhang et al. 2020). Pan et al. (2016) prepared multifunctional cotton with antibacterial property and hydrophobicity by using polymeric *N*-halamine precursor modified graphene oxide. The functional fabrics achieved antibacterial efficacy and self-cleaning ability (Pan et al. 2016). Zhang et al. (2019) synthesized *N*-halamine copolymers and coated them on cotton fabrics. The prepared fabrics showed excellent antibacterial efficacy which could inactivate six logs of bacteria within 1 min (Zhang et al. 2019). Improving the hydrophobicity of cotton fabrics can enhance their resistance to bacterial adhesion and antibacterial durability. Some studies for preparing antibacterial cotton fabrics with hydrophobicity have been reported. Yang et al (2020) manufactured an non-fluorinated superhydrophobic and antibacterial cotton through in situ growing zeolitic imidazolate framework-8 (ZIF-8) and being coated with polydimethylsiloxane (PDMS) (Yang et al. 2020). The obtained cotton fabric showed superhydrophobicity and high antibacterial activity against *E. coli* and *S. aureus*. Ma (2019) et al. prepared antibacterial and hydrophobic cotton fabrics with *N*-halamine siloxanes, ZnO, and silane precursors via the ultrasonic-assisted dipping-padding assembly technique. The coated cotton fabrics showed good hydrophobicity and antibacterial efficacy. 69% of the chlorine was retained after the equivalent of 25 machine washes, indicating the excellent durability (Ma et al. 2019).

To extend the usefulness of cellulose textiles, creating a cotton fabric with multifunctionality is one of the future research goals. The studies of cotton fabrics with effectively flame retardancy, and simultaneously providing antibacterial and hydrophobic properties have been rarely reported until now. Herein, a water-soluble flame retardant and antibacterial polymer P(AA-ADMH) was synthesized by introducing *N*-halamine structure into PAAs. In order to achieve efficient flame retardant and antibacterial modified cotton fabrics, P(AA-ADMH) was reacted with PA and γ-aminopropyl triethoxysilane (APS) to achieve modification via LBL self-assembly method. The *N*-halamine structure of P(AA-ADMH) created the main antibacterial component. Meanwhile, P(AA-ADMH), PA and APS impacted P/N/Si synergistic flame retardancy of fabrics. The flame-retardant performance and mechanism of the modified cotton fabrics were studied. Antibacterial properties, hydrophobicity, mechanical properties and durability of the modified fabrics were also characterized.

## Experimental

### Materials

Glycine (G), lithium hydroxide monohydrate ($LiOH{\cdot}H_2O$), sodium hypochlorite solution (NaClO),

**Scheme 1** Synthesis of P(AA-ADMH)

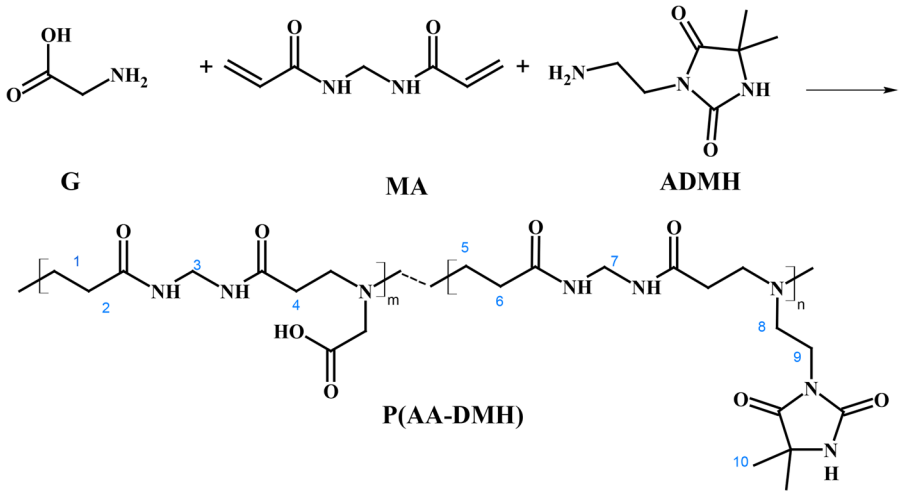


sodium hydroxide (NaOH) and sulfuric acid ($H_2SO_4$) were purchased from Sinopharm Group Chemical Reagent (Shanghai, China) Co., Ltd. Phytic acid (PA), N, N'-methylenebisacrylamide (MA) and γ-Aminopropyl triethoxysilane (APS) were purchased from Beijing Bailingwei Technology (Beijing, China) Co., Ltd. Cotton fabrics (110 g/m$^2$) were obtained from Zhejiang Guandong Textile Dyeing Garment (Zhejiang, China) Co., Ltd.

## Synthesis of P(AA-ADMH)

Synthesis of P(AA-ADMH) is shown in Scheme 1: Typically, $LiOH{\cdot}H_2O$ (0.01 mol, 0.42 g) was dissolved in 5.79 mL deionized water (DI). Then G (0.008 mol, 0.6 g) and ADMH (0.002 mol, 0.34 g, prepared as per the methods reported in a previous study (Jiang et al. 2016) were introduced to the mixture, stirred for 30 min at 25 °C. Furthermore, MA (0.01 mol, 1.54 g) was added to the mixture, stirred at 50 °C until the mixture became a clear transparent solution. Finally, the product P(AA-ADMH) solution was obtained after stirring at 25 °C for 48 h. Then the product was diluted to 100 mL with DI, and ultra-filtered through a membrane.

## Preparation of the modified cotton fabrics

Cotton fabrics were pre-treated with 1.0 wt% NaOH aqueous solution. The P(AA-ADMH) solution was diluted to 10 wt% for application to modify the cotton fabrics. The cationic solutions of LBL consisted of 5wt% APS aqueous solution (pH = 3.4, adjusted by 5 mol/L $H_2SO_4$ aqueous solutions); 10 wt% P(AA-ADMH) aqueous solution and 2 wt% PA aqueous solution were prepared as anionic solution.

One-bilayer for P(AA-ADMH)/APS cotton (Scheme 1): The cotton fabrics were exposed to 5 wt% APS for 20 min, washed and dried at 80 °C. Then cotton fabrics were exposed to 10 wt% P(AA-ADMH) for 10 min, washed and dried at 80 °C.

One-bilayer for P(AA-ADMH)/PA/APS cotton (Scheme 2): 1 BL of P(AA-ADMH)/APS cotton was exposed to 5 wt% APS for 20 min, washed and dried at 90 °C, then the modified fabric was exposed to exposed to in 2 wt% PA for 10 min, washed and dried at 90 °C.

## Chlorination of the modified cotton fabrics

The P(AA-ADMH)/APS cotton and P(AA-ADMH)/PA/APS cotton were submerged in 10% NaClO aqueous solution (regulated with 10% $H_2SO_4$ aqueous solution, pH = 7) for 1 h, washed and dried at 50 °C for 2 h. The chlorine content of samples were analysed via iodine/thiosulfate titration (Ma et al. 2019).

## Analytical measurements

Structural analysis: The P(AA-ADMH) was freeze-dried for nuclear magnetic resonance ($^1$H NMR) and Fourier transform infrared spectroscope (FTIR) tests. The $^1$H-NMR analysis was recorded on Bruker Avance III 400 NMR spectrometer. The solvent was

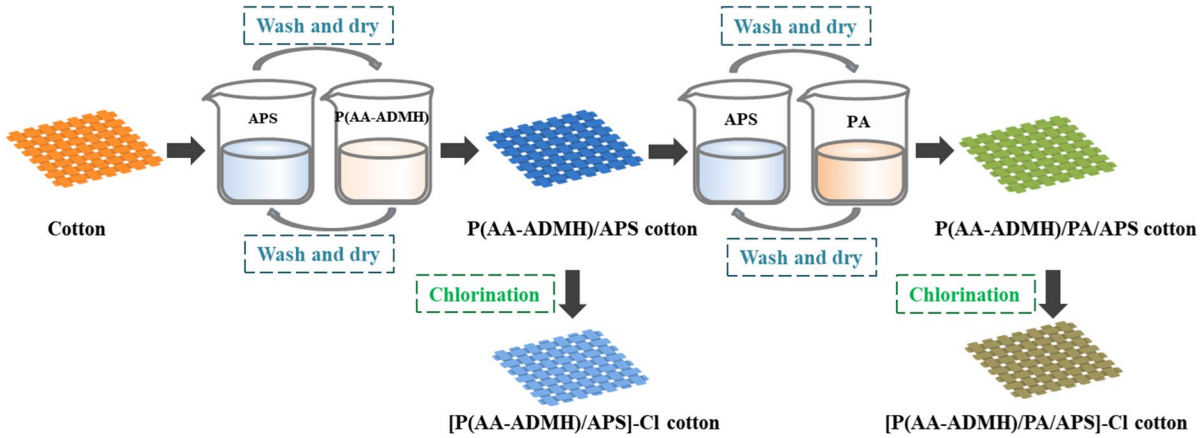


**Scheme 2** Schematic illustration of the preparation of the modified cotton fabrics

$D_2O$ (99.9%). (1.34 ppm: H10 and H11; 2.67 ppm: H2 and H6; 3.37 ppm: H1, H5 and 3 0.62 ppm: H4, H8 and H9; 4.53 ppm: H3 and H7). The FTIR analysis was recorded on Fourier infrared spectrometer (Nicolet Avatar370, USA). The morphology of the samples was recorded on Hitachi SU-1510 scanning electron microscopy (SEM, Japan) which was connected energy dispersive X-ray spectrometer (EDS). The samples were sputtered with gold for 60 s. The test voltage of SEM was 5 kV, and the test voltage of EDS was 15 kV. X-ray diffraction (XRD) of various samples was recorded on X-ray diffractor (Bruker D2 PHASER, Germany) to obtain 2750 counts in the range of 5°-60° with a step size of 0.02°. The complete fabrics were used as the test samples. X-ray photoelectron spectra (XPS, Thermo Scientific K-Alpha, UK) were performed to study the contents of the elements on the samples. The radiation power was 15 kW. The dimensions of samples were 5 mm × 5 mm. The water contact angles were evaluated by PT-602A contact angle analyzer (China), and 4 μL of DI was used as testing liquid. Thermogravimetric (TG) analysis was conducted with a TA Instruments Q500 thermal analyzer in a temperature range (30–700 °C) at 10 °C / min in static $N_2$ atmosphere, and each sample was 5 mg.

According to GB / T 17591–2006 standard, LOI was conducted on a JF-3 type digital limiting oxygen index analyzer instrument (China). According to GB / T 5455–2014 standard, vertical burning tests were recorded in a vertical flame chamber. Cone calorimeter test (CCT) was investigated by using an FTT Fire Testing Technology (UK). The heat flux was 35 kw / $m^2$. Thermogravimetric analysis coupled with Fourier Transform infrared spectroscopy (TG-FTIR, BR UKER TGA-IR) was performed to evaluate the thermogravimetric properties of the modified cotton fabrics in a temperature range (50–800 °C) at 10 °C/min in static $N_2$ atmospheres.

Antibacterial activity evaluation: The antibacterial efficiencies of control cotton, $[P(AA\text{-}ADMH)/APS]_{15}$-Cl cotton and $[P(AA\text{-}ADMH)/PA/APS]_{15}$-Cl cotton were evaluated by contact test and bacterial biofilm test. Escherichia coli (*E. coil*) and Staphylococcus aureus (*S. aureus*) were set as the model strain for the test. The method of contact test was assessed by AATCC Test Method 100–2004 (Kong et al. 2021b). Two 2.54 cm × 2.54 cm samples were contact with 25 μL bacterial inoculum with 30, 60, and 120 min. Then the bacteria were extracted from the samples and incubated at 37 °C for 24 h. The number of bacterial colonies was counted for biocidal assessment. The inhibitory effect of the samples for bacterial biofilm was assessed by bacterial biofilm-controlling test. The samples were exposed to the bacterial inoculum for 2 h, then the bacteria were removed by rinsing with phosphate buffered saline (PBS) and incubated in broth at 37 °C for 24 h. Part of the samples were immersed into 5 mL PBS, vortexed for 2 min. Then, the bacteria were inoculated on nutrient agar medium (NAM) plates for CFU determination. Part of the samples were exposed to glutaraldehyde solution (3 wt%) at 4 °C for 12 h to fix the bacteria,

then dehydrated with ethanol solutions (30%, 50%, 75%, 90%, and 100%) and dried for SEM observation.

Tensile tests were recorded on YG026D-250 electronic universal testing machine (China) with 10 mm/min strain rate. The washing durability of chlorinated modified samples was conducted under AATCC 61–2006 standard.

## Results and discussion

### Characterization of P(AA-ADMH)

$^1$H NMR spectrum of P(AA-ADMH) is shown in Fig. 1a. The signals of 2.67 ppm and 3.37 ppm were assigned to -$CH_2$- of P(AA-ADMH) (Xia et al. 2022), and the peak at 4.53 ppm to the N-$CH_2$-N group. The peaks at 3.4–4.3 ppm correspond to -$CH_3$ from P(AA-ADMH). Furthermore, one peak located at 3.62 ppm was assigned to the N-$CH_2$- group of P(AA-ADMH) (Kang et al. 2013). The FTIR spectra of P(AA-ADMH) is shown in Fig. 1b. The peaks at 3056 $cm^{-1}$ and 1532 $cm^{-1}$ were ascribed to the stretching vibration and formation vibration of N–H (Arioli et al. 2020), respectively. The peaks at 1721 $cm^{-1}$ and 1622 $cm^{-1}$ corresponding to the stretching vibration of C=O, were attributed to ADMH and G (Yin et al. 2016). The peak at 3241 $cm^{-1}$ was ascribed to the stretching vibration of C-H. The peaks at 1382 $cm^{-1}$ and 1231 $cm^{-1}$ corresponding to C-H formation vibration, were due to P(AA-ADMH) polymer. The peaks at 1337 $cm^{-1}$ and 1108 $cm^{-1}$ were attributed to the stretching vibration of C-O and C–C, respectively. The results of $^1$H NMR and FTIR indicated that a successful reaction happened between MA with G and ADMH.

### Characterization of the modified cotton fabrics

Firstly, XRD patterns of control cotton, [P(AA-ADMH)/APS]$_{15}$-Cl cotton and [P(AA-ADMH)/PA/APS]$_{15}$-Cl cotton are shown in Fig. 2a. Compared to control cotton, there was no significant change observed for the non-crystalline phase structure of the modified samples. According to Fig. 2a, all samples showed four peaks at the 2θ values around 15°, 17°, 23° and 34°, which were assigned to the (1–10), (110), (200), and (004) crystal planes of cellulose (French 2014; Gao et al. 2019). These peaks of the modified cotton fabrics shifted slightly, indicating cotton fibers swelled in NaOH and cellulose I structure was partially destroyed (Zhou et al. 2020). The results of the XRD analyses indicated that the treatment did not substantially affect the crystal structures of the cotton fabrics. Furthermore, XPS spectra in Fig. 1b showed O1s (534.02 eV) and C1s (284.09 eV) signals for control cotton, while the spectrum of [P(AA-ADMH)/APS]$_{15}$-Cl cotton exhibited N1s, Si2s, Si2p and Cl2p peaks at 400.1 eV, 152.1 eV, 101.3 eV and 202.2 eV(Jiang

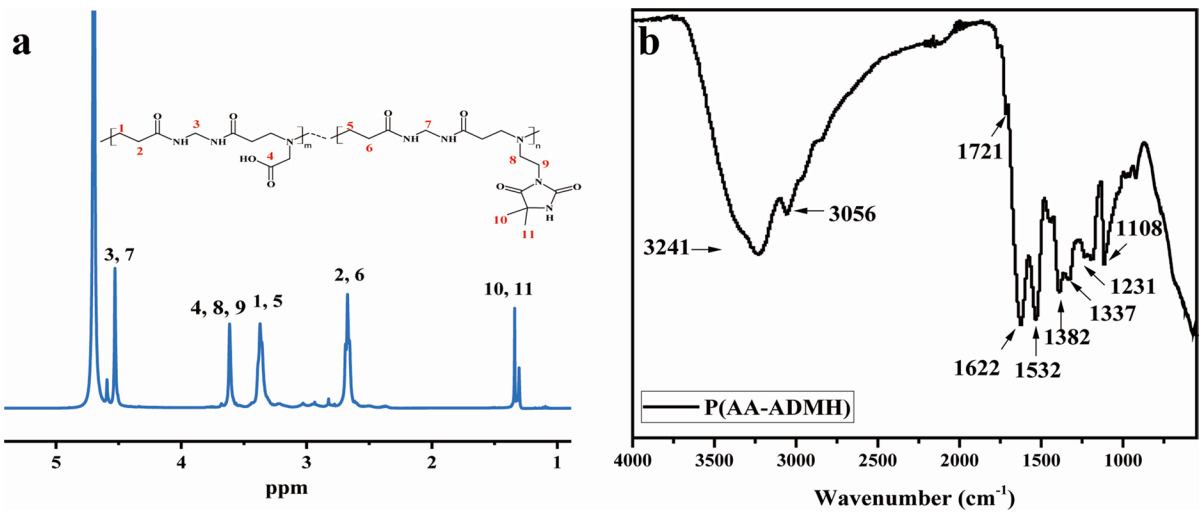


**Fig. 1** $^1$H-NMR spectrum **a** and FTIR spectrum **b** of P(AA-ADMH)

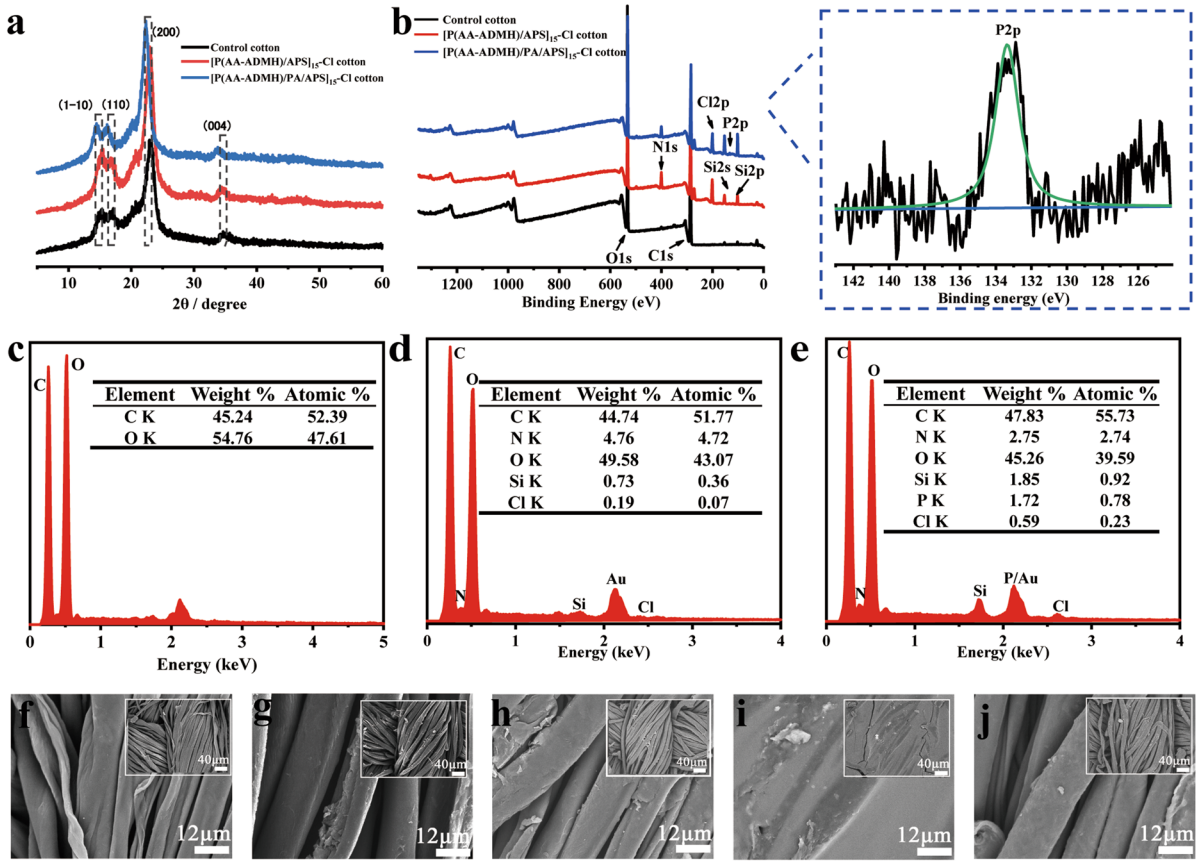


**Fig. 2** XRD and XPS spectra of control and modified samples (**a**) and (**b**). EDS spectra of control cotton (**c**), [P(AA-ADMH)/APS]$_{15}$-Cl cotton (**d**) and [P (AA-ADMH)/PA/APS]$_{15}$-Cl cotton (**e**). SEM images (×500, ×2000): Control cotton (**f**), P(AA-ADMH)/APS]$_{15}$ cotton (**g**), [P(AA-ADMH)/APS]$_{15}$-Cl cotton (**h**), P(AA-ADMH)/PA/APS]$_{15}$ cotton (**i**) and [P(AA-ADMH)/PA/APS]$_{15}$-Cl cotton (**j**)

et al. 2019), proving the successful modification of control cotton. Moreover, the peak at 133.4 eV (P2p) in the spectrum of [P(AA-ADMH)/PA/APS]$_{15}$-Cl cotton was due to the presence of PA (Li et al. 2019a).

To explore the elements of the modified samples, EDS was carried out. As depicted in Figs. 2c, d and e, the surface elemental composition of [P(AA-ADMH)/APS]$_{15}$-Cl cotton showed the typical N and Si elements of P(AA-ADMH) and APS, and [P(AA-ADMH)/PA/APS]$_{15}$-Cl cotton exhibited P element of PA. Furthermore, the morphology of the control and modified samples was investigated via SEM, (Figs.2f-j). The surface of the control cotton was glossy. After modification, the fabrics clearly exhibited a layer of coating.

## Thermal properties

TG and DTG curves are shown in Fig. 3, and the relevant TG data are summarized in Table S1. The first 5% weight loss ($T_{5\%}$) of control cotton resulted from evaporation of water. Remarkably, the temperature at $T_{5\%}$ of two modified cotton fabrics obviously decreased, which was due to the lower degradation temperature of P (AA-ADMH) and PA (Lin et al. 2019). The main weight loss of the control cotton in temperature range of 292–381 °C, the maximum weight loss rate ($R_{max}$) of 2.5%/°C at 355 °C was due to the decomposititon of cellulose (Wang et al. 2022b). It was worth mentioning that the modified cotton fabrics displayed almost the same thermal behaviors, and presented lower values of $R_{max}$

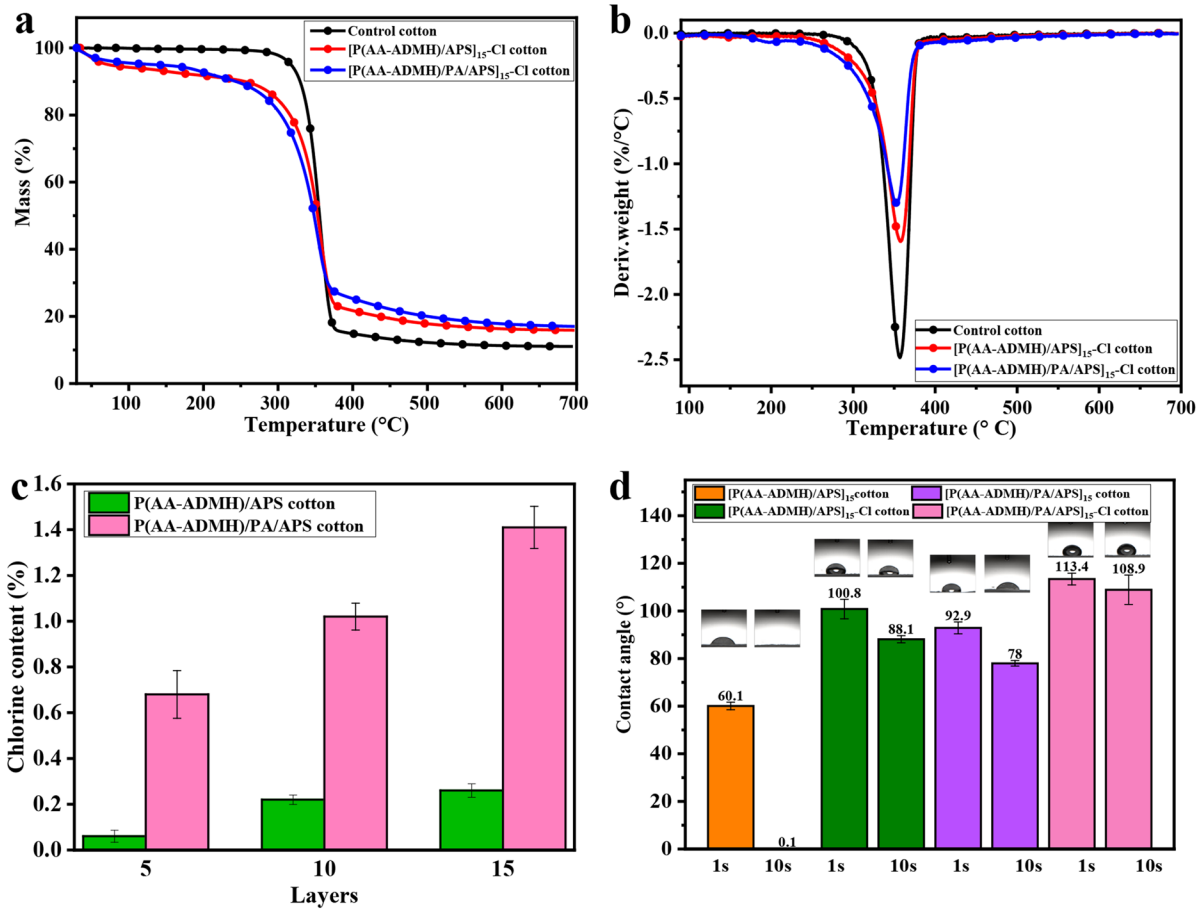


**Fig. 3** TG and DTG curves of control and the modified samples (**a**) and (**b**). Chlorine content of the modified samples (**c**). WCA of the modified cotton samples (**d**)

than that of control cotton. In addition, the rate of char residue at 700 °C of [P(AA-ADMH)/APS]$_{15}$-Cl cotton increased from 11.1% to 15.9%, which was mainly due to the high thermal stability of inorganic silica generated from the degraded APS (Wang et al. 2022a). When heating, PA was cracked into polyphosphoric acid and phosphoric acid, propelling the pyeolysis and carbonation of cellulose and suppressing production of L-glucose (de Oliveira et al. 2021b). Therefore, the char residue of [P(AA-ADMH)/PA/APS]$_{15}$-Cl cotton was higher than [P(AA-ADMH)/APS]$_{15}$-Cl cotton. These results could prove that the synergistic effect of P(AA-ADMH) and PA could further prevented the thermal degradation.

## Chlorine content

Generally, the chlorine content directly shows the load of *N*-halamine and the antibacterial property of the modified fabrics. As shown in Fig. 3c, with increasing the numbers of layers, the chlorine content gradually increased. In addition, compared to [P(AA-ADMH)/APS]-Cl cotton, the [P(AA-ADMH)/PA/APS]-Cl cotton exhibited a higher chlorine content, which might be due to the more APS layers in resulting in P(AA-ADMH) being strongly bound to the cotton fabrics (Mostofi Sarkari et al. 2019). [P(AA-ADMH)/PA/APS]$_{15}$-Cl cotton with the highest chlorine content were used for further testing.

Static hydrophobic properties

The WCA value and test images are displayed in Fig. 3d. Regular cotton fabrics (the WCA is around 0°) are considered highly hydrophilic due to the existence of abundant hydroxyl groups in the cellulosic chemical structure (Maia et al. 2022). According to Fig. 3d, with 1 s contact time, the WCA of $[P(AA\text{-}ADMH)/APS]_{15}$ cotton and $[P(AA\text{-}ADMH)/PA/APS]_{15}$ cotton were 61.0° and 92.9°. On the one hand, the dehydration condensation of APS layers that occurred in the cotton fabrics could reduce the hydroxyl groups on the cotton surface (Cheng et al. 2015), contributing to the increase of WCA. On the other hand, according to SEM results (Figs. 2f-g), the surface roughness of the modified cotton fabrics was increased, which promoted by self-assembled layers deposition, resulted in higher WCA of the modified samples. Meanwhile, the WCA of the modified fabrics increased further after chlorination, the reason might be that N–H bonds [P(AA-ADMH)] changed to N-Cl bonds, leading to the reduction of hydrogen bonds in cotton fabrics. According to the images of Fig. 3d, most of the water was still retained on the surface of the modified fabrics over 10 s. It demonstrated that the load of the self-assembled layers rendered cotton fabrics some hydrophobicity (Cao et al. 2022; Kong et al. 2021).

Flame retardant properties

To analyze the flame retardant properties of the modified cotton fabrics, LOI and vertical burning tests were carried out (Fig. 4 and Table S2). Compared to the regular cotton (the LOI value is 18.0%), the LOI of [P(AA-ADMH)/PA/APS]-Cl cotton increased significantly with increasing number of the layers, especially for 15 BL (27.3%). Generally, after ignition, the regular cotton burned rapidly within a time of 12 s and flame was extinguished without residue. In contrast, $[P(AA\text{-}ADMH)/APS]_{15}$-Cl cotton was carbonized completely during flame combustion and smoldering with a decreased of combustion rate, as schematized in Fig. 4a. According to Table S2, [P(AA-ADMH)/PA/APS]-Cl cotton with 5 BL could self-extinguish once the fire source was removed. For 15 BL, the sample had no both afterflame time and afterglow time, the value of char length was 12.2 cm.

CCT was performed to simulate a realistic fire scene, and further evaluated the flammability performance of the modified samples. Critical combustion data are reported in Fig. 5 and Table S3. For control cotton, typical peak heat release rate (PHRR) was 117 kW/m$^2$, and total heat release (THR) was 2.2 MJ/m$^2$. In contrast, for the $[P(AA\text{-}ADMH)/APS]_{15}$-Cl cotton, the PHRR and THR decreased by 8.5% and 22.7%, respectively. Increasing the layers of PA further decreased the PHRR and THR values, 29.1% and 31.8% reduction were observed for $[P(AA\text{-}ADMH)/PA/APS]_{15}$-Cl cotton. The results demonstrated that the fire threat of the modified cotton fabrics was reduced and could extend fire escape time (de Oliveira et al. 2021a). The time to ignition (TTI) value of $[P(AA\text{-}ADMH)/PA/APS]_{15}$-Cl cotton was 3 s, which was lower than that of control cotton (7 s). This phenomenon was accordance with the results of TG measurements. During combustion, PA firstly

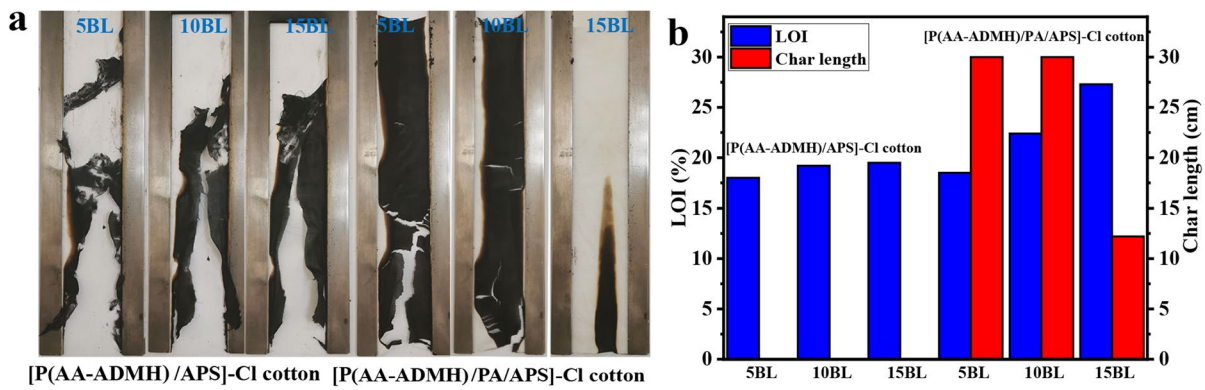


**Fig. 4** Digital images of the modified samples through vertical burning tests (**a**). LOI and char length of the modified samples (**b**)

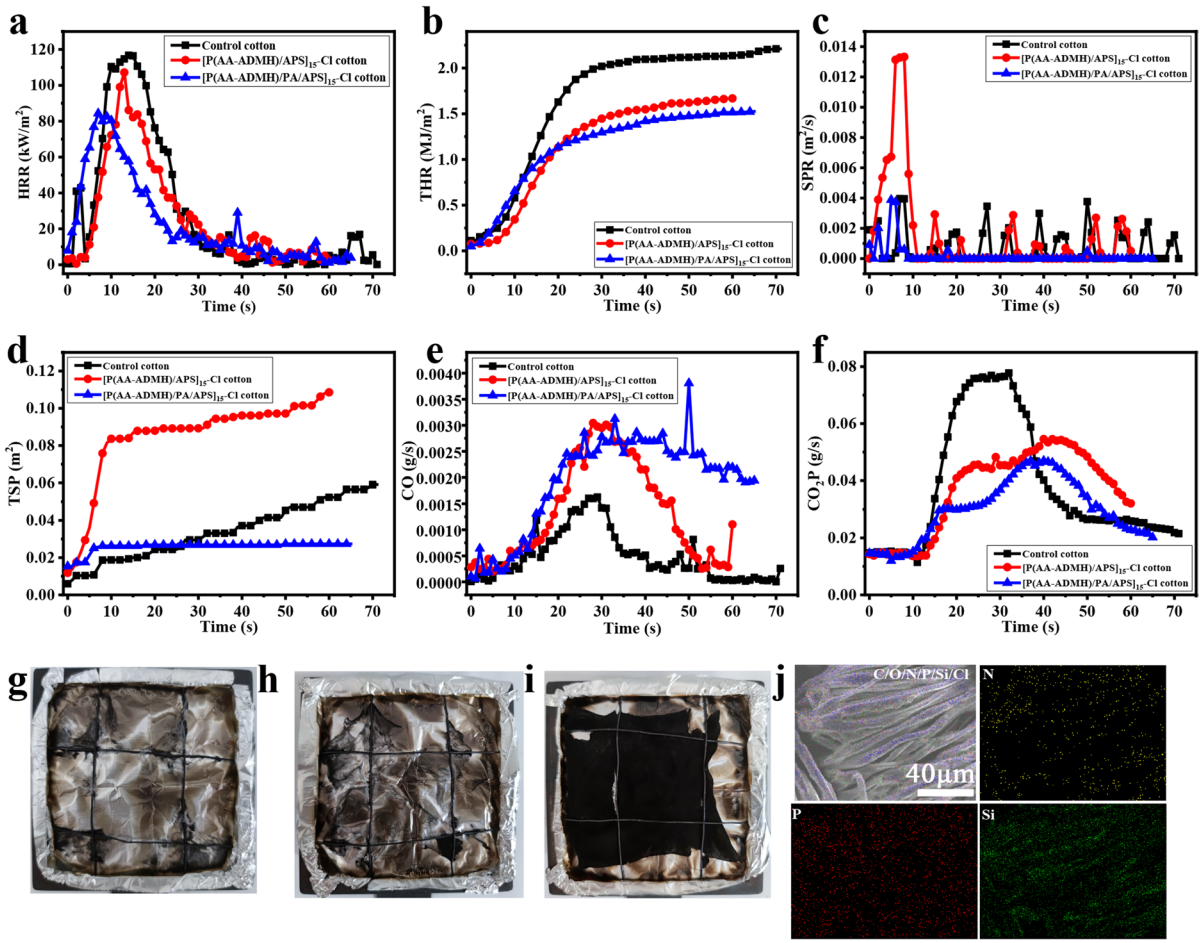


**Fig. 5** CCT data: HRR (**a**); THR (**b**); SPR (**c**); TSP (**d**); COP (**e**) and $CO_2P$ (**f**). Digital photographs of control and modified samples after cone calorimeter test: control cotton (**g**); [P(AA-ADMH)/APS]$_{15}$-Cl cotton (**h**) and [P(AA-ADMH)/PA/APS]$_{15}$-Cl cotton (i). Mapping images for the char of [P(AA-ADMH)/PA/APS]$_{15}$-Cl cotton (j)

decomposed, which lead to the earlier pyrolysis of [P(AA-ADMH)/PA/APS]$_{15}$-Cl cotton.

The smoke release threats the safety of evacuation greatly. As shown in Fig. 5c, the values of smoke production rate (SPR) and total smoke production (TSP) of [P(AA-ADMH)/APS]$_{15}$-Cl cotton dramatically increased. Comparatively, both SPR and TSP values of [P(AA-ADMH)/PA/APS]$_{15}$-Cl cotton obviously reduced, due to the deposition of PA. In other words, [P(AA-ADMH)/PA/APS]$_{15}$-Cl cotton achieved great fire safety, and had a lower smoke emission as well. The CO production rate (COP, Fig. 5e) values of [P(AA-ADMH)/APS]$_{15}$-Cl cotton and [P(AA-ADMH)/PA/APS]$_{15}$-Cl cotton increased, and the $CO_2$ production rate ($CO_2P$, Fig. 5f) values decreased, which was caused by the low combustion efficiency of the modified cotton fabrics. This indicated that the modified layers were conductive to hindering the release of combustion component formed in condensed phase decomposition (Chen et al. 2019). According to the data in Table S3, the char residue of P(AA-ADMH)/PA/APS]$_{15}$-Cl cotton increased from 0.1 to 17.1 wt%. Moreover, P, N, and Si elements (Fig. 5j) were observed on the [P(AA-ADMH)/PA/APS]$_{15}$-Cl cotton after burning. The digital photographs in Figs. 5g-i for the residues of samples after the CCT test confirmed the above results. As shown in Fig. 5, control cotton burnt completely, meanwhile, [P(AA-ADMH)/PA/APS]$_{15}$-Cl cotton formed continuous and compact char residue.

Flame retardant mechanism

To discover the flame retardant mechanism of the modified samples, TG-IR and the morphology of residues was conducted. The thermal decomposition products of modified and control cotton fabrics were investigated by TG-FTIR in the temperature range of 50–800 °C. As revealed in Figs. 6a-c, comparison

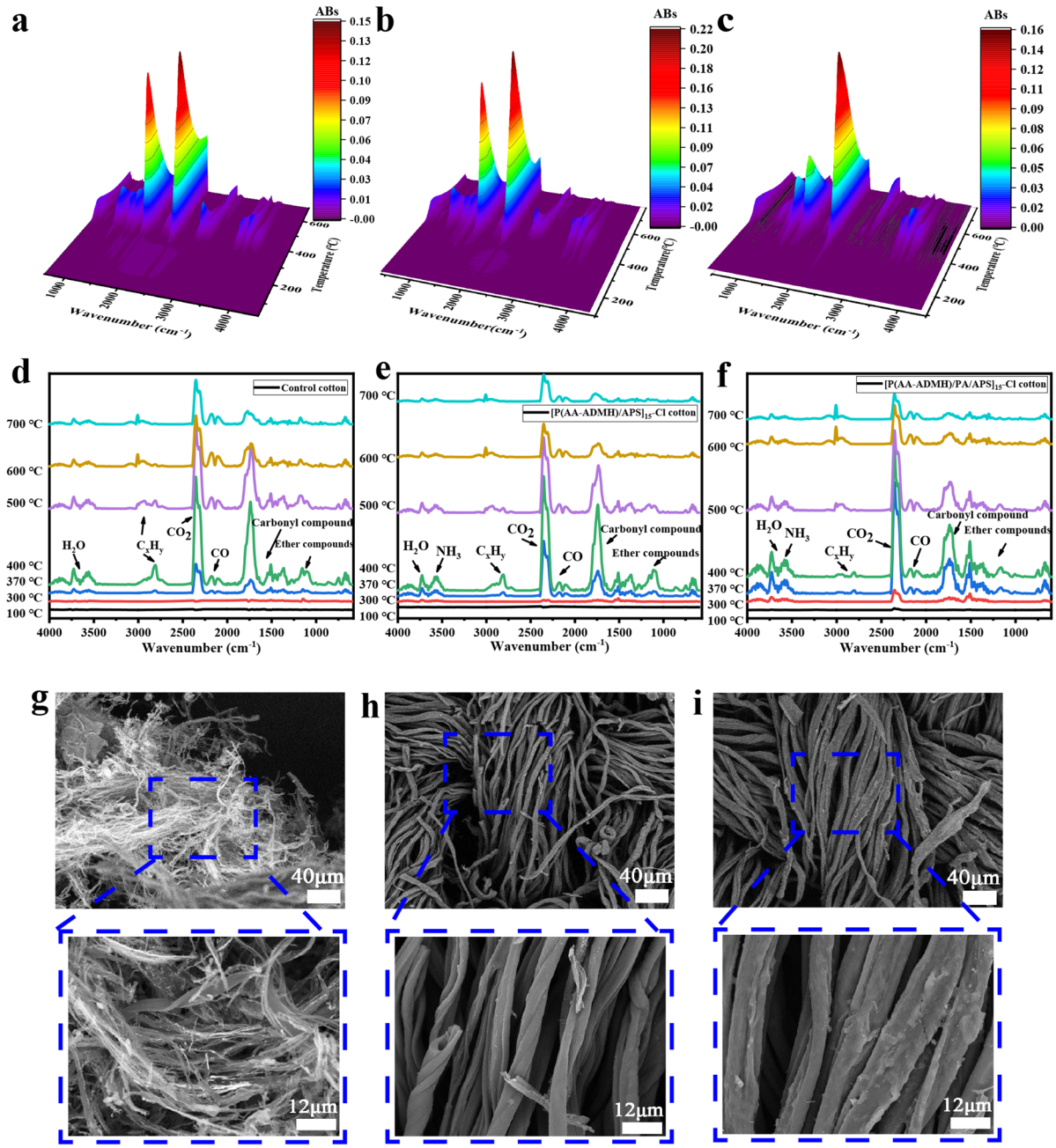


**Fig. 6** 3D TG-FTIR curves: (**a**), P(AA-ADMH)/APS]-Cl cotton (**b**) and [P(AA-ADMH)/PA/APS]-Cl cotton (**c**). FTIR spectra of pyrolysis volatile products: cotton fabrics (**d**), P(AA-ADMH)/APS]-Cl cotton (**e**) and [P(AA-ADMH)/PA/APS]-Cl cotton (**f**). SEM images (×500,×2000) of samples: Control cotton (**g**), $P(AA\text{-}ADMH)/APS]_{15}$-Cl cotton (**h**) and $[P(AA\text{-}ADMH)/PA/APS]_{15}$-Cl cotton (**i**)

with the control cotton, the absorption positions of FTIR peaks [P(AA-ADMH)/APS]$_{15}$-Cl cotton and [P (AA-ADMH)/PA/APS]$_{15}$-Cl cotton presented similar, with only difference in peak intensity, which was caused by the change of the released gas (Wang et al. 2018a). The FT-IR curves of samples at different temperature are shown in Figs. 6 d-e, to verify the decomposition products further. As shown in Fig. 6d, the control cotton began to decomposed of at around 370 °C, with emerging the characteristic absorption peaks which were owing to $H_2O$ (3764–3459 $cm^{-1}$), carbonyl compounds (2864–2765 $cm^{-1}$), $CO_2$ (2403–2246 $cm^{-1}$), CO (2183-2111 $cm^{-1}$) and carbonyl groups (1740 $cm^{-1}$) (Rao et al. 2021). From Fig. 6d, the absorption intensity of the peaks at 2809 $cm^{-1}$(carbonyl compounds) from the modified cotton fabrics (Figs. 6e-f) were obviously decreased, indicating that [P(AA-ADMH)/APS]$_{15}$-Cl cotton and [P(AA-ADMH)/PA/APS]$_{15}$-Cl cotton produced fewer volatile products containing hydrocarbon during the pyrolysis process. For the modified samples, the strength of 3584 $cm^{-1}$ ($NH_3$) and 3731 $cm^{-1}$ ($H_2O$) peaks were increased, suggesting the higher release of $NH_3$ and $H_2O$ from the modified samples (Zheng et al. 2016). In addition, compared with control and [P(AA-ADMH)/APS]$_{15}$-Cl cotton, the peaks of ether compounds and carbonyl compound (which belong to flammable substances) from [P(AA-ADMH)/PA/APS]$_{15}$-Cl cotton were significantly reduced.

The morphology of the char residue after the vertical burning test was observed to further discover flame resistance mechanism of the modified fabrics. As could be observed in Fig. 6g, the fibers of control cotton were loose, and the structure was broken. However, the SEM images (Fig. 6h-i) of [P(AA-ADMH)/APS]$_{15}$-Cl cotton and [P(AA-ADMH)/PA/APS]$_{15}$-Cl cotton presented the image of the complete structure and shape of fibers. After combustion, the fibers of [P(AA-ADMH)/APS]$_{15}$-Cl cotton showed rough surfaces but loose structures, with severe shrinkage and fractures, which resulted from unsatisfactory flame retardancy of P(AA-ADMH) and APS. As for the [P(AA-ADMH)/PA/APS]$_{15}$-Cl cotton, the fibers stayed fully compact and almost integral, with the char layer being thicker and more condensed. This structure was able to lower combustible gases release and to block the heat exchange, thereby [P(AA-ADMH)/PA/APS]$_{15}$-Cl cotton have great flame retardant property (Rosace et al. 2017). This phenomenon was due to the cooperation of PA and APS. During combustion, cotton fibers were promoted the dehydration and carbonization as a result of the pyrolysis of PA. Meanwhile, Si compound of APS could contribute to form more stable carbon layer contained silicon (Jin et al. 2023).

Thus, P, N and Si elements of modified system improved flame retardant property of cotton fabrics via two pathways. In the gas phase, modified cotton fabrics released some non-flammable gas which could dilute flammable volatiles. In the condensed phase, the modified cotton fabrics shield heat transfer and lowered oxygen passage via promoting the formation of a dense and complete residue structure.

## Antibacterial activities

According to Fig. 7a, the unchlorinated modified cotton fabrics did not display antimicrobial activity within 120 min. While, [P(AA-ADMH)/APS]$_{15}$-Cl cotton and [P(AA-ADMH)/PA/APS]$_{15}$-Cl cotton exhibited high antibacterial efficiencies, and over 90% against *E. coli* and *S. aureus* within 30 min. The antibacterial rate of [P(AA-ADMH)/PA/APS]$_{15}$-Cl cotton was 100% against *S. aureus* and *E. coli* within 60 min and 120 min, respectively. According to the literature (Zheng et al. 2021), the oxidative chlorine ($Cl^+$) reacted with appropriate receptors in the bacteria, leading to intracellular content leakage, which finally caused the bacteria to be inactivated. Therefore, the oxidative chlorine provided by *N*-halamine attributed to the potent antibacterial property of the modified fabrics (Yang et al. 2021). The results of biofilm-controlling test are shown in Fig. 7c-d, [P(AA-ADMH)/APS]$_{15}$-Cl cotton and [P(AA-ADMH)/PA/APS]$_{15}$-Cl cotton could effectively inhibit the adherence of bacteria. The control cotton showed a recoverable *E. coli* and *S. aureus* level with $2.40 \pm 0.33 \times 10^6$ CFU/mL and $2.53 \pm 0.50 \times 10^6$ CFU/mL, respectively. After treatment with [P(AA-ADMH)/APS]$_{15}$-Cl cotton for 2 h, 72.21% and 47.44% of *E. coli* and *S. aureus* were decreased, respectively. For [P(AA-ADMH)/PA/APS]$_{15}$-Cl cotton, the adherent level of *E. coli* and *S. aureus* decreased significantly by 83.33% and 99.99%, respectively. To further investigate the antibacterial mechanism, morphological studies of control and modified cotton fabrics contacted with bacteria were conducted. According to Figs. 7e and j,

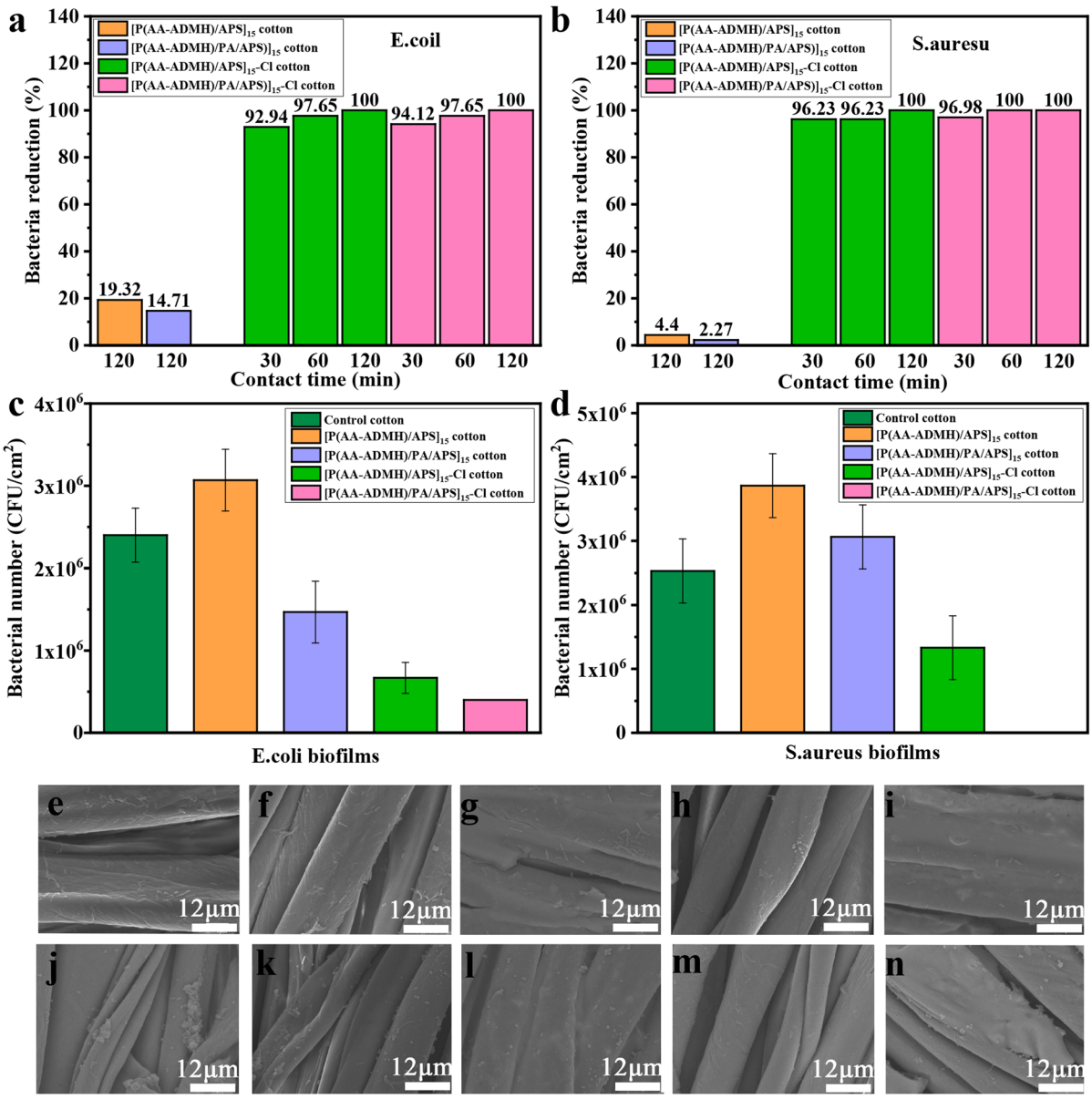


**Fig. 7** Biocidal activities of the control and modified samples against *E. coli* (Inoculum concentration: $5.25\times10^6$ CFU) (**a**) and *S. aureus* (Inoculum concentration: $3.96\times10^6$ CFU) (**b**). Biofilms controlling ability of: *E. coli* (**c**) and *S. aureus* (**d**). SEM images of bacterial biofilm(×2000). *E. coli*: Control cotton (**e**), $[P(AA\text{-}ADMH)/APS]_{15}$ cotton (**f**), $P(AA\text{-}ADMH)/PA/APS]_{15}$ cotton (**g**), $[P(AA\text{-}ADMH)/APS]_{15}$-Cl cotton (**h**), $[P(AA\text{-}ADMH)/PA/APS]_{15}$-Cl cotton (**i**); *S. aureus*: Control cotton (**j**), $[P(AA\text{-}ADMH)/APS]_{15}$ cotton (k), $P(AA\text{-}ADMH)/PA/APS]_{15}$ cotton (**l**), $[P(AA\text{-}ADMH)/APS]_{15}$-Cl cotton (**m**), $[P(AA\text{-}ADMH)/PA/APS]_{15}$-Cl cotton (**n**)

the regular cotton was covered with a large amount of layered of *E. coli* and *S. aureus*, while, $[P(AA\text{-}ADMH)/APS]_{15}$-Cl cotton and $[P(AA\text{-}ADMH)/PA/APS]_{15}$-Cl cotton appeared relatively clean, evidencing that the modification of cotton fabrics

effectively reduced the bacteria adhesion and the related biofilm formation.

### Washing durability

To verify the washing durability of the modified cotton fabrics, the flame retardant and antibacterial properties of $[P(AA\text{-}ADMH)/APS]_{15}$-Cl cotton and $[P(AA\text{-}ADMH)/PA/APS]_{15}$-Cl cotton were evaluated after 5 and 10 washing cycle time. The LOI and chlorine content is shown in Fig. 8a. After washing for 5 cycles, the chlorine content of $[P(AA\text{-}ADMH)/APS]_{15}$-Cl cotton had decreased from 0.26% to 0.03%, $[P(AA\text{-}ADMH)/PA/APS]_{15}$-Cl cotton had decreased from 1.41% to 0.11%. During the washing test, the N-Cl bonds in modified samples decomposed, leading to decrease of the chlorine content. Furtherly, the chlorine content of modified cotton fabrics was nearly undetectable after 10 washing cycles. However, most initial chlorine content could be regenerated with a re-chlorination process by exposure to NaClO solution. After 10 washing cycles, the LOI of $[P(AA\text{-}ADMH)/PA/APS]_{15}$-Cl cotton reduced from 27.3% to 24.3% which was indicated that the durability of modified sample could be preserved in part.

### Mechanical characterization

The mechanical properties of the modified cotton fabrics were evaluated via tensile strength tests. As presented in Fig. 8c-d, the tensile strength of modified cotton fabrics was retained by around 90% in warp

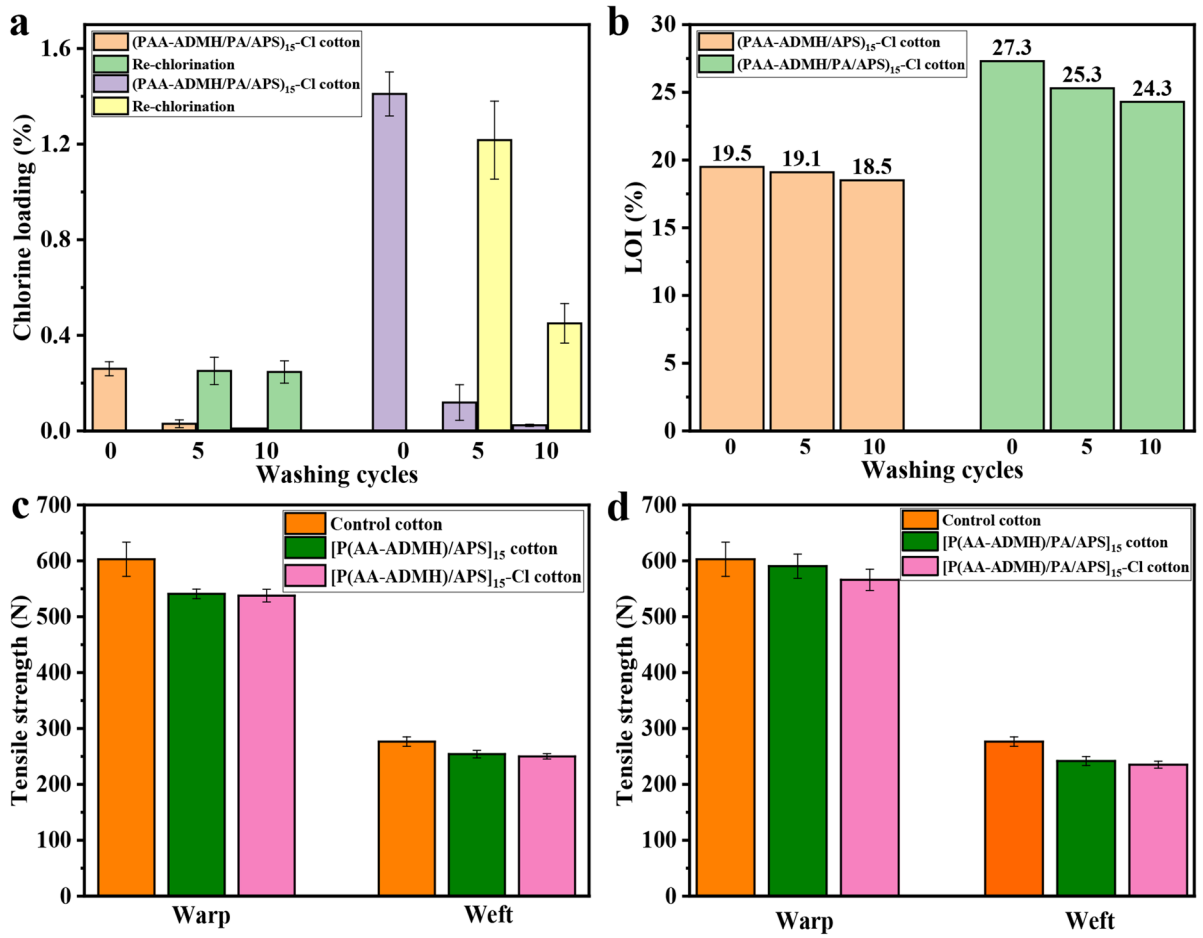


**Fig. 8** Results of washing (AATCC 61–1996): Chlorine loading (**a**) and LOI (**b**). Tensile strength of the modified samples (**c**) and (**d**)

and weft directions. The decline could be the results of the weak acidity of modification conditions and high temperature (Xu et al. 2019). From Fig. 8c-d, the tensile strength of the unchlorinated and chlorinated modified samples was almost the same; these results indicated that the chlorination treatment hardly affected the tensile properties of cotton fabrics.

## Conclusions

In summary, novel flame retardant, antibacterial cotton fabrics with increased hydrophobicity were prepared through LBL self-assembly method with synthesized P(AA-ADMH), PA and APS. After the modification, phosphorus, nitrogen and silicon elements were verified on cotton fabrics. The modified cotton fabrics $[P(AA\text{-}ADMH)/PA/APS]_{15}$-Cl cotton had a LOI value of 27.3%, exhibiting good flame-retardant performance, and self-extinguishing capabilities were proved by vertical combustion. Owing to the *N*-halamine structure, the modified cotton fabrics inactivated 100.0% of *E. coli* and *S. aureus* within 120 min. In addition, modified cotton fabrics presented some hydrophobicity, which contributed to the decrease of the bacterial adsorption and favored the antibacterial property. These multifunctional cotton fabrics show potential applications as protective textiles.

**Acknowledgments** The authors gratefully acknowledge the financial support from the Fundings.

**Author contributions** XC: Data curation, Conceptualization, Methodology, Investigation, Writing-original draft, Formal analysis, Validation. FD: Methodology, Software. SZ: Visualization, Formal analysis. YL: Conceptualization, Investigation, Funding acquisition. XH: Conceptualization, Resources, Writing-review & editing. XR: Conceptualization, Resources, Supervision, Writing-review & editing, Funding acquisition.

**Funding** This work is supported by Postgraduate Research & Practice Innovation Program of Jiangsu Province (KYCX22_2355), the Natural Science Foundation of Jiangsu Province (BK20190606), and China Postdoctoral Science Foundation (2020M681486).

**Data availability** Not applicable.

**Declarations**

**Conflict of interest** The authors declare that they have no known competing financial interests or personal relationships that could have appeared to influence the work reported in this paper.

**Ethics approval and consent to participate** This research work did not involve any human or animal participants.

**Consent for publication** The authors hereby consent to publication of the present research work in this journal, if selected for publication.

## References

Arioli M, Manfredi A, Alongi J, Ferruti P, Ranucci E (2020) Highlight on the mechanism of linear polyamidoamine degradation in water. Polymers (Basel). https://doi.org/10.3390/polym12061376

Bentis A, Boukhriss A, Grancaric AM, El Bouchti M, El Achaby M, Gmouh S (2019) Flammability and combustion behavior of cotton fabrics treated by the sol gel method using ionic liquids combined with different anions. Cellulose 26(3):2139–2153. https://doi.org/10.1007/s10570-018-2206-4

Cao Y, Zhou M, Wang SF, Fu HQ (2022) Superhydrophobic and flame retardant polydimethylsiloxane coatings with layered double hydroxide and ammonium polyphosphate. Prog Org Coat. https://doi.org/10.1016/j.porgcoat.2022.107117

Chen T, Hong J, Peng CH, Chen GR, Yuan CH, Xu YT, Zeng BR, Dai LZ (2019) Superhydrophobic and flame retardant cotton modified with DOPO and fluorine-silicon-containing crosslinked polymer. Carbohydr Polym 208:14–21. https://doi.org/10.1016/j.carbpol.2018.12.023

Cheng XL, Li R, Du JM, Sheng JF, Ma KK, Ren XH, Huang TS (2015) Antimicrobial activity of hydrophobic cotton coated with *N*-halamine. Polym Adv Technol 26(1):99–103. https://doi.org/10.1002/pat.3426

de Oliveira CRS, Batistella MA, Lourenço LA, de Souza SMAGU, de Souza AAU (2021) Cotton fabric finishing based on phosphate/clay mineral by direct-coating technique and its influence on the thermal stability of the fibers. Prog Org Coat. https://doi.org/10.1016/j.porgcoat.2020.105949

de Oliveira CRS, Batistella MA, Ulson SMAG, de Souza AAU (2021) Functionalization of cellulosic fibers with a kaolinite-$TiO_2$ nano-hybrid composite via a solvothermal process for flame retardant applications. Carbohydr Polym. https://doi.org/10.1016/j.carbpol.2021.118108

French AD (2014) Idealized powder diffraction patterns for cellulose polymorphs. Cellulose 21(2):885–896. https://doi.org/10.1007/s10570-013-0030-4

Gao D, Li YJ, Lyu B, Lyu LH, Chen SW, Ma JZ (2019) Construction of durable antibacterial and anti-mildew cotton fabric based on P(DMDAAC-AGE)/Ag/ZnO composites. Carbohydr Polym 204:161–169. https://doi.org/10.1016/j.carbpol.2018.09.087

Jiang ZM, Liu Y, Li R, Ren XH, Huang TS (2016) Preparation of antibacterial cellulose with a

monochloro-s-triazine-based *N*-halamine biocide. Polym Adv Technol 27(4):460–465. https://doi.org/10.1002/pat.3691

Jiang ZM, Li H, He YW, Liu Y, Dong CH, Zhu P (2019) Flame retardancy and thermal behavior of cotton fabrics based on a novel phosphorus-containing siloxane. Appl Surf Sci 479:765–775. https://doi.org/10.1016/j.apsusc.2019.02.159

Jin X, Li WN, Wang SH, Li YY, Yang CH, Lu Z, Dong CH (2023) Developing flame-retardant, antibacterial cotton fabric by incorporating a linear polysiloxane-based coating. Ind Crop Prod. https://doi.org/10.1016/j.indcrop.2022.115934

Kang ZZ, Zhang B, Jiao YC, YiH Xu, He QZ, Liang J (2013) High-efficacy antimicrobial cellulose grafted by a novel quaternarized *N*-halamine. Cellulose 20(2):885–893

Kong Q, Li ZG, Ding F, Ren XH (2021) Hydrophobic *N*-halamine based POSS block copolymer porous films with antibacterial and resistance of bacterial adsorption performances. Chem Eng J 410:128407

Li P, Wang B, Xu YJ, Jiang ZM, Dong CH, Liu Y, Zhu P (2019a) Ecofriendly flame-retardant cotton fabrics: preparation, flame retardancy, thermal degradation properties, and mechanism. ACS Sustain Chem Eng 7(23):19246–19256. https://doi.org/10.1021/acssuschemeng.9b05523

Li SS, Lin XH, Liu Y, Li R, Ren XH, Huang TS (2019b) Phosphorus-nitrogen-silicon-based assembly multilayer coating for the preparation of flame retardant and antimicrobial cotton fabric. Cellulose 26(6):4213–4223. https://doi.org/10.1007/s10570-019-02373-5

Li P, Wang B, Liu YY, Xu YJ, Jiang ZM, Dong CH, Zhang L, Liu Y, Zhu P (2020) Fully bio-based coating from chitosan and phytate for fire-safety and antibacterial cotton fabrics. Carbohydr Polym 237:116173. https://doi.org/10.1016/j.carbpol.2020.116173

Li N, Kang GW, Liu H, Qiu WW, Wang Q, Liu L, Wang XL, Yu JY, Li FX, Wu DQ (2022) Fabrication of eco-friendly and efficient flame retardant modified cellulose with antibacterial property. J Colloid Interface Sci 618:462–474. https://doi.org/10.1016/j.jcis.2022.03.078

Lin DM, Zeng XR, Li HQ, Lai XJ, Wu TY (2019) One-pot fabrication of superhydrophobic and flame-retardant coatings on cotton fabrics via sol-gel reaction. J Colloid Interface Sci 533:198–206. https://doi.org/10.1016/j.jcis.2018.08.060

Ma W, Li L, Ren X, Huang TS (2019) Rational design of cotton substrates with enhanced UV–blocking, high antibacterial efficiency and prominent hydrophobicity. Cellulose 26(9):5757–5768

Maia MT, Noronha VT, Oliveira NC, Alves AC, Faria AF, Martinez DTS, Ferreira OP, Paula AJ (2022) Silica nanoparticles and surface silanization for the fabrication of water-repellent cotton fibers. ACS Appl Nano Mater. https://doi.org/10.1021/acsanm.1c03346

Makhlouf G, Abdelkhalik A, Ameen H (2021) Synthesis of a novel highly efficient flame-retardant coating for cotton fabrics with low combustion toxicity and antibacterial properties. Cellulose 28(13):8785–8806. https://doi.org/10.1007/s10570-021-04076-2

Manfredi A , Carosio F , Ferruti P , Ranucci E , Alongi J (2018) Linear polyamidoamines as novel biocompatible phosphorus-free surface-confined intumescent flame retardants for cotton fabrics. Polym Degrad Stabil 151:52–64. https://doi.org/10.1016/j.polymdegradstab.2018.02.020

Mostofi Sarkari N, Doğan Ö, Bat E, Mohseni M, Ebrahimi M (2019) Assessing effects of (3-aminopropyl)trimethoxysilane self-assembled layers on surface characteristics of organosilane-grafted moisture-crosslinked polyethylene substrate: a comparative study between chemical vapor deposition and plasma-facilitated in situ grafting methods. Appl Surf Sci. https://doi.org/10.1016/j.apsusc.2019.143751

Mu T, Pan NY, Wang YF, Ren XH, Huang TS (2018) Antibacterial coating of cellulose by Iso-bifunctional reactive N-halamine with the dyeing process of reactive dye. Fiber Polym 19(11):2284–2289

Nabipour H, Wang X, Rahman MZ, Song L, Hu Y (2020) An environmentally friendly approach to fabricating flame retardant, antibacterial and antifungal cotton fabrics via self-assembly of guanazole-metal complex. J Clean Prod. https://doi.org/10.1016/j.jclepro.2020.122832

Pan NY, Liu Y, Fan XY, Jiang ZM, Ren XH, Liang J (2016) Preparation and characterization of antibacterial graphene oxide functionalized with polymeric *N*-halamine. J Mater Sci 52(4):1996–2006. https://doi.org/10.1007/s10853-016-0488-1

Pan Y, Liu LX, Wang X, Song L, Hu Y (2018) Hypophosphorous acid cross-linked layer-by-layer assembly of green polyelectrolytes on polyester-cotton blend fabrics for durable flame-retardant treatment. Carbohydr Polym 201:1–8. https://doi.org/10.1016/j.carbpol.2018.08.044

Rao WH, Shi JJ, Yu CB, Zhao HB, Wang YZ (2021) Highly efficient, transparent, and environment-friendly flame-retardant coating for cotton fabric. Chem Eng J. https://doi.org/10.1016/j.cej.2021.130556

Rosace G, Colleoni C, Trovato V, Iacono G, Malucelli G (2017) Vinylphosphonic acid/methacrylamide system as a durable intumescent flame retardant for cotton fabric. Cellulose 24(7):3095–3108

Tian CC, Wu F, Jiao WL, Liu XY, Yin X, Si Y, Yu JY, Ding B (2021) Antibacterial and antiviral *N*-halamine nanofibrous membranes with nanonet structure for bioprotective applications. Compos Commun. https://doi.org/10.1016/j.coco.2021.100668

Wang DF, Zhong L, Zhang C, Li SN, Tian PX, Zhang FX, Zhang GX (2018a) Eco-friendly synthesis of a highly efficient phosphorus flame retardant based on xylitol and application on cotton fabric. Cellulose 26(3):2123–2138. https://doi.org/10.1007/s10570-018-2193-5

Wang DF, Zhong L, Zhang C, Zhang FX, Zhang GX (2018b) A novel reactive phosphorous flame retardant for cotton fabrics with durable flame retardancy and high whiteness due to self-buffering. Cellulose 25(10):5479–5497

Wang B, Li P, Xu YJ, Jiang ZM, Dong CH, Liu Y, Zhu P (2020) Bio-based, nontoxic and flame-retardant cotton/alginate blended fibres as filling materials: Thermal degradation properties, flammability and flame-retardant mechanism. Compos Part B Eng. https://doi.org/10.1016/j.compositesb.2020.108038

Wang SH, Sun L, Li YY, Wang HX, Liu J, Zhu P, Dong CH (2021) Properties of flame-retardant cotton fabrics:

Combustion behavior, thermal stability and mechanism of Si/P/N synergistic effect. Ind Crop Prod. https://doi.org/10.1016/j.indcrop.2021.114157

Wang SH, Sun L, Li YY, Wang HX, Ji L, Zhu P, Dong CH (2021b) Properties of flame-retardant cotton fabrics: Combustion behavior, thermal stability and mechanism of Si/P/N synergistic effect. Ind Crop Prod 173:114157

Wang LJL, Xu YJ, Liu Y, Zhu P (2022a) Flame retardation of polyester/cotton blended fabrics via intumescent sol-gel coatings. Polym Degrad Stabil 204:110115

Wang CB, Wu J, Miao ZW, Zhang XF, Yan DP, Liu WW, Wu DZ, Wu ZP (2022) Permanent P/N-rich polymeric coating capable of extinguishing flame on cotton fabrics. Prog Org Coat. https://doi.org/10.1016/j.porgcoat.2022.107004

Xia L, Dai J, Wang XH, Xue MJ, Xu YT, Yuan CH, Dai LZ (2022) Facile fabrication of multifunctional cotton fabric by AgNC@boronate polymer/crosslinked chitosan. Carbohydr Polym. https://doi.org/10.1016/j.carbpol.2022.119384

Xu F, Zhong L, Xu Y, Zhang C, Wang P, Zhang FX, Zhang GX (2019) Synthesis of three novel amino acids-based flame retardants with multiple reactive groups for cotton fabrics. Cellulose 26(12):7537–7552

Xu DH, Wang SJ, Hu JW, Liu Y, Jiang ZM, Zhu P (2021) Enhancing antibacterial and flame-retardant performance of cotton fabric with an iminodiacetic acid-containing *N*-halamine. Cellulose 28(5):3265–3277. https://doi.org/10.1007/s10570-021-03716-x

Yang YY, Guo ZP, Huang W, Zhang SY, Huang JJ, Yang HJ, Zhou YS, Xu WL, Gu SJ (2020) Fabrication of multifunctional textiles with durable antibacterial property and efficient oil-water separation via in situ growth of zeolitic imidazolate framework-8 (ZIF-8) on cotton fabric. Appl Surf Sci 503:144079

Yang ZM, Ren XH, Liu Y (2021) *N*-halamine modified ceria nanoparticles: Antibacterial response and accelerated wound healing application via a 3D printed scaffold. Compos Part B Eng. https://doi.org/10.1016/j.compositesb.2021.109390

Yin ML, Chen XL, Li R, Huang D, Fan XY, Ren XH, Huang TS (2016) Preparation and characterization of antimicrobial PVA hybrid films with *N*-halamine modified chitosan nanospheres. J Appl Polym Sci. https://doi.org/10.1002/app.44204

Zhang D, Williams BL, Shrestha SB, Nasir Z, Becher EM, Lofink BJ, Santos VH, Patel H, Peng X, Sun L (2017) Flame retardant and hydrophobic coatings on cotton fabrics via sol-gel and self-assembly techniques. J Colloid Interface Sci 505:892–899. https://doi.org/10.1016/j.jcis.2017.06.087

Zhang FX, Gao WW, Jia YL, Lu Y, Zhang GX (2018) A concise water-solvent synthesis of highly effective, durable, and eco-friendly flame-retardant coating on cotton fabrics. Carbohydr Polym 199:256–265. https://doi.org/10.1016/j.carbpol.2018.05.085

Zhang SM, Demir B, Ren XH, Worley SD, Broughton RM, Huang TS (2019) Synthesis of antibacterial *N*-halamine acryl acid copolymers and their application onto cotton. J Appl Polym Sci. https://doi.org/10.1002/app.47426

Zhang SM, Li L, Ren XH, Huang TS (2020) *N*-halamine modified multiporous bacterial cellulose with enhanced antibacterial and hemostatic properties. Int J Biol Macromol 161:1070–1078

Zhang AN, Liu BW, Zhao HB, Wang YZ (2022) Eco-friendly and durable flame-retardant coating for cotton fabrics based on dynamic coordination of Ca2+-tannin acid. Prog Org Coat. https://doi.org/10.1016/j.porgcoat.2022.106964

Zheng DD, Zhou JF, Zhong L, Zhang FX, Zhang GX (2016) A novel durable and high-phosphorous-containing flame retardant for cotton fabrics. Cellulose 23(3):2211–2220

Zheng YX, Pan NY, Liu Y, Ren XH (2021) Novel porous chitosan/*N*-halamine structure with efficient antibacterial and hemostatic properties. Carbohydr Polym 253:117205. https://doi.org/10.1016/j.carbpol.2020.117205

Zhou TC, Xu HD, Cai L, Wang JJ (2020) Construction of antiflame network structures in cotton fabrics with pentaerythritol phosphate urea salt and nano SiO2. Appl Surf Sci 507:145175